High Power Laser Science and Engineering, (2024), Vol. 12, e80, 7 pages.
doi:10.1017/hpl.2024.67

HIGH POWER LASER SCIENCE AND ENGINEERING

RESEARCH ARTICLE

Post-compression of the GW-level femtosecond pulse in a solid-state multi-pass cell

Liya Shen[1,2], Jiajun Song[1], Yujie Peng[1], Guangxin Luo[1,3], Yinfei Liu[1,4], Jianyu Sun[1,4], and Yuxin Leng[1]

[1]*State Key Laboratory of High Field Laser Physics and CAS Center for Excellence in Ultra-intense Laser Science, Shanghai Institute of Optics and Fine Mechanics (SIOM), Chinese Academy of Sciences (CAS), Shanghai, China*

[2]*School of Physical Science and Technology, ShanghaiTech University, Shanghai, China*

[3]*Department of Optics and Optical Engineering, University of Science and Technology of China, Hefei, China*

[4]*Center of Materials Science and Optoelectronics Engineering, University of Chinese Academy of Sciences, Beijing, China*

(Received 23 July 2024; revised 2 September 2024; accepted 24 September 2024)

Abstract

We demonstrate the post-compression of the GW-level femtosecond pulse in a solid-state multi-pass cell (MPC) by the pre-chirp management method. When the laser pulse is positively pre-chirped, the 200 μJ 170 fs input pulse is compressed to 163 μJ 44 fs at the output, corresponding to a transmission of 81% and a pulse shortening factor of 3.86. When the laser pulse is negatively pre-chirped, the spectral evolution, as the pulse propagates in the MPC, is characterized and, eventually, the pulse duration is compressed to 51 fs, corresponding to a pulse shortening factor of 3.3. After the driving laser goes through the pre-chirp managed MPC device, the power stability and beam quality are almost preserved. The experimental results offer a viable path toward the post-compression of high-peak-power laser pulses.

Keywords: post-compression; pre-chirped management; femtosecond pulse

1. Introduction

High-power, ultrashort femtosecond lasers are versatile tools for the research of high harmonic generation[1,2], time resolved pump–probe experiments[3,4] and material processing[5,6]. Ytterbium (Yb)-doped gain media have great potential for radiating high-power femtosecond lasers due to their low quantum defects, long upper-state lifetimes and high-power laser diode pumping configurations. Nevertheless, the pulse duration of Yb-doped amplifiers is typically longer than 100 fs due to the finite gain bandwidth and gain narrowing effect during the amplification process.

To shorten the pulse duration, spectral broadening via self-phase modulation (SPM) followed by chirp removal, also known as post-compression, could be a feasible approach. Various post-compression devices have been proposed and implemented, such as hollow core fiber[7], solid thin plates[8–10], Herriott-type multi-pass cells (MPCs)[11–15], photonic crystal fiber[16,17] and Kagome photonic crystal fiber[18,19]. Among these, the MPC is the latest post-compression approach, initially demonstrated by Schulte *et al.* in 2016[11]. The MPC stands out because of its high efficiency, simple configuration, sufficient clear apertures, unprecedented robustness and impressive power and energy handling capabilities. It consists of two concave mirrors and Kerr media positioned between them. The Kerr media can be solid plates or inert gas. Figure 1 presents an overview of the input pulse parameters for MPC devices utilizing different Kerr media. In addition, there are two comprehensive review papers covering the majority of MPC research[20,21]. It is clear that MPC devices with different Kerr media are suitable for post-compression of laser pulses with different peak powers. So far, the peak power of the laser pulse employing a solid-state MPC for post-compression of the pulse duration has been 5.6 MW–1.6 GW[2,12], while more solid-state

Correspondence to: J. Song, Y. Peng and Y. Leng, State Key Laboratory of High Field Laser Physics and CAS Center for Excellence in Ultra-intense Laser Science, Shanghai Institute of Optics and Fine Mechanics (SIOM), Chinese Academy of Sciences (CAS), Shanghai 201800, China. Emails: songjiajun@siom.ac.cn (J. Song); yjpeng@siom.ac.cn (Y. Peng); lengyuxin@mail.siom.ac.cn (Y. Leng)

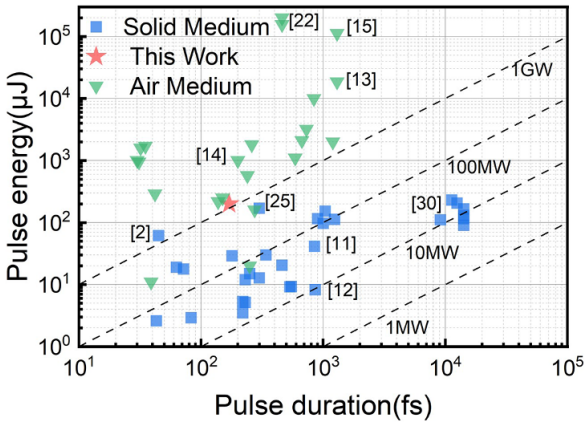

Figure 1. Overview of the input pulse parameter for the MPC with different Kerr media.

MPCs are adaptable for post-compression of 10 MW-level laser pulses to avoid ionization of the Kerr media. Further, the peak power of the laser pulse employing a gas-filled MPC for post-compression is 485 MW–434 GW[15,22], while more gas-filled MPCs handle laser pulses with more than 1 GW peak power because of the higher gas ionization threshold. However, gas-filled MPCs involve bulky vacuum equipment and are cumbersome to operate. While GW-level compression has been achieved in solid-state MPCs[2], the energy scaling may still pose a risk of damage unless the MPC setups are expanded. Therefore, to realize post-compression of the GW-level laser pulse with a simpler solid-state MPC, it is necessary to reduce the peak power of the laser pulse firstly. One approach is to decrease the pulse energy through pulse division[23]. Another is to increase the pulse width, which can be realized by the pre-chirp management approach[24]. While keeping the pulse energy constant, the pulse duration of the laser pulse is stretched prior to injection into the MPC, resulting in a significant degradation of the peak power. As a result, the nonlinearity during the laser pulse propagation in the Kerr medium is clearly mitigated.

In this paper, we propose and perform post-compression of the GW-level femtosecond laser pulse in a solid-state MPC through pre-chirp management. The pulse duration of the laser pulse with a peak power of up to 1.1 GW is pre-chirped from 170 to 600 fs before it is coupled into the solid-state MPC. When the laser pulse is positively pre-chirped, the spectral broadening with a factor of 5.6 and pulse compression with a factor of 3.86 are experimentally realized. In addition, when the laser pulse is negatively pre-chirped, the spectral evolution of the laser pulse during propagation in the MPC is characterized. The spectral bandwidth is compressed first for six times propagating inside the MPC, followed by subsequent spectral broadening. Eventually, a 4.4-fold spectral broadening and a 3.3-fold pulse compression are achieved. The power stability and beam quality of the driving laser are almost preserved after the pre-chirp managed MPC device.

2. Experimental setup

Figure 2(a) depicts the experimental setup of our pre-chirp managed post-compression system operating in ambient air. An Yb-doped solid-state amplifier is employed as the laser source, which emits 6 W average power at a repetition rate of 30 kHz. The central wavelength and spectral bandwidth (full width at half maximum, FWHM) of the laser source are 1037 and 11.3 nm, respectively. The pulse duration of the driving laser is initially 170 fs assuming a Gaussian pulse shape, as shown in Figure 2(b). Hence, the peak power of the driving laser reaches 1.1 GW. In addition, the pulse duration can be stretched by introducing positive or negative dispersion. A half wave plate (HWP) and a thin film polarizer (TFP) form an adjustable attenuator to control the power injected into the MPC. The laser beam is mode-matched to the MPC using three lenses (L1–L3). The MPC is composed of two concave mirrors (CM1 and CM2) with a diameter of 2 inches and a radius of curvature of 300 mm. They are coated for high reflection and low dispersion from 950 to 1120 nm. The distance between CM1 and CM2 is approximately 550 mm, corresponding to an eigenmode beam radius of 0.57 and 0.17 mm on CM1 and CM2 and in the middle of the MPC, respectively. The laser beam is coupled in and out of the MPC unit by two rectangular mirrors with the size of 3 mm × 15 mm. Two 2 mm thick fused silica (FS) plates are exploited as the Kerr media, positioned 12.5 cm from the MPC mirrors, and the beam radius in the FS plates is estimated to be 0.34 mm. The laser beam is aligned to propagate through 41 times inside the MPC, corresponding to a propagation length of 0.164 m in the FS and 22.4 m in free space. The FS length, position and roundtrips are optimized to balance the desired spectral broadening with operational safety while maximizing power efficiency and compactness. The spectrally broadened pulses from the MPC subsequently undergo chirp removal by using chirped mirrors.

As mentioned by Chen and Chang[24], the spectral broadening capability of the laser pulse is diminished for both positively and negatively pre-chirped pulses. Hence, the amount of pre-chirped group delay dispersion (GDD) should be carefully set to maintain the spectral broadening capability of the MPC while avoiding laser-induced damage and the occurrences of some unwanted nonlinearities. Here, we refer to Raab *et al.*[25] to degrade the peak power of the laser pulse to about 300 MW. The pulse duration is pre-chirped to 600 fs by increasing the positive GDD of the driving laser, as presented in Figure 2(c). At this condition, the peak power of the pulse is 313 MW. It is enabled to execute post-compression in a solid-state MPC device[25]. We infer the laser pulse has a GDD of 3.5×10^4 fs^2.

https://doi.org/10.1017/hpl.2024.67 Published online by Cambridge University Press

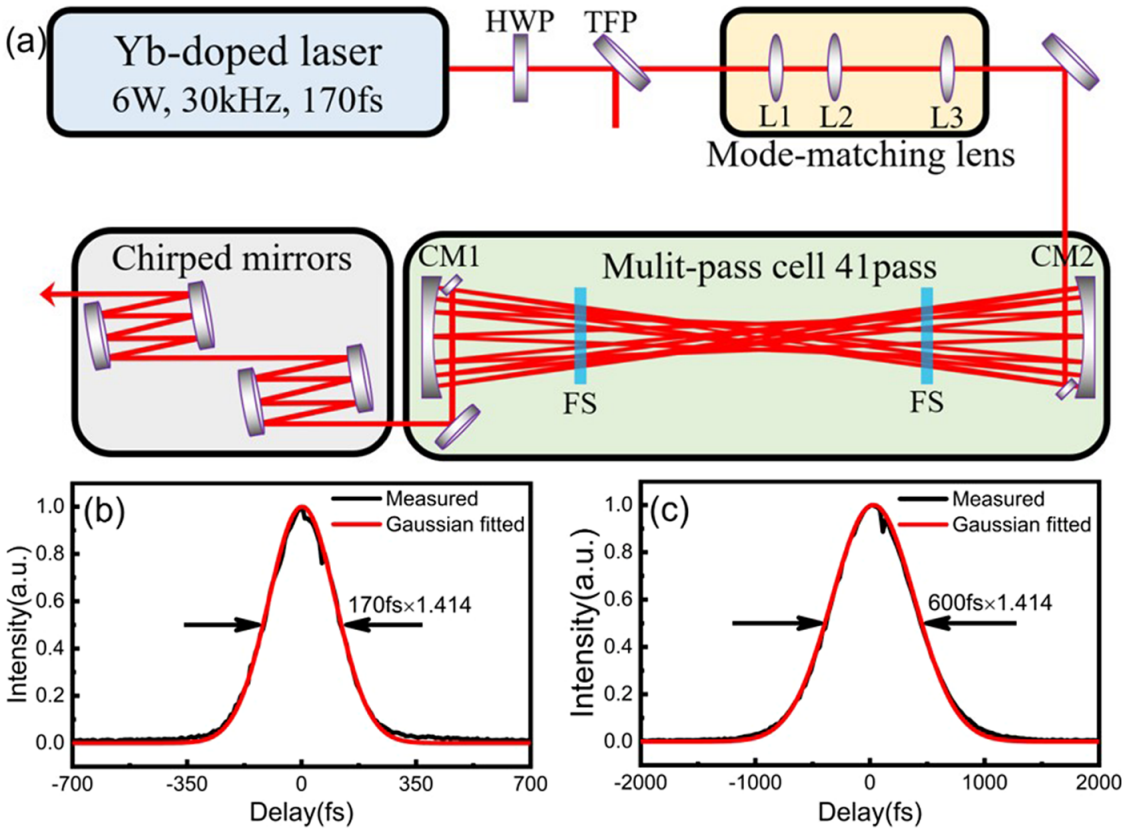

Figure 2. (a) Schematic layout of the pre-chirp management nonlinear compression setup. HWP, half wave plate; TFP, thin film polarizer; L1–L3, lenses; CM1 and CM2, concave mirrors; FS, fused silica plate. (b) Pulse duration of the driving laser. (c) Pulse duration after pre-chirping.

3. Results and discussion

The average powers before and after the MPC unit are 6 and 4.9 W, respectively, corresponding to a transmission of 81%. This efficiency is considered low for a single-stage MPC device, which is attributed to the low transmittance of the FS plates' coating. As the plates are removed from the system, the transmittance is enhanced to 95%. A small amount of nonlinearity is accumulated as the pulse passes through the FS plates once. After passing through the MPC unit, significant nonlinear phase shifts accumulate, leading to dramatic spectral broadening. The spectral bandwidth from the MPC is broadened to 63.1 nm at the intensity of half the outer spectral maxima, as shown in Figure 3(a) (black line), which yields a broadening factor of 5.4. The theoretically calculated spectral broadening results[26] of the

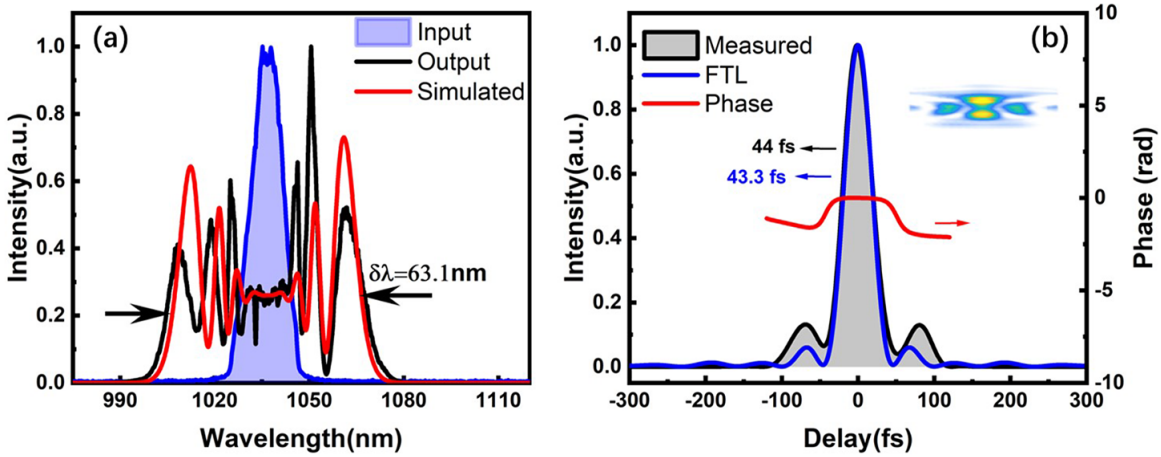

Figure 3. (a) Input spectrum (blue line), output spectrum of the positively pre-chirped MPC (black line) and its corresponding theoretical simulation (red line). (b) Retrieved temporal intensity (black line), phase (red line) and FTL pulse width (blue line) with an inset of the measured FROG trace.

https://doi.org/10.1017/hpl.2024.67 Published online by Cambridge University Press

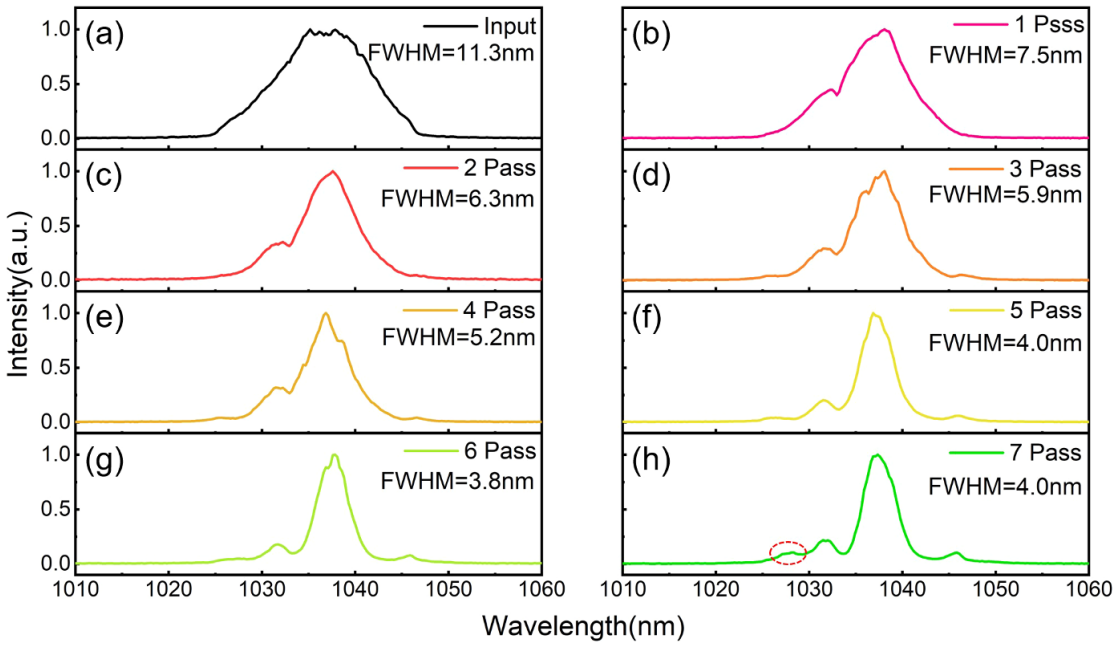

Figure 4. Spectral evolution when the laser pulse is negatively pre-chirped as it propagates in the MPC. (a)–(g) The spectrum progressively narrows with increasing passes through the MPC. (h) The spectrum begins to broaden.

positively pre-chirped pulse are also shown in Figure 3(a) (red line), which fit well with the experimental results. The Fourier transform limit (FTL) pulse duration of the broadened spectrum is calculated to be 43.3 fs. Due to the intensity modulation of the broadened spectrum, approximately 89% of the pulse energy is concentrated in the main peak of the FTL pulse. The chirped mirrors are employed to remove the positive chirp of the laser pulses. When the compensated GDD reaches –6200 fs^2, a retrieved pulse width of 44 fs is obtained via second harmonic generation-frequency resolved optical gating (SHG-FROG), as shown in Figure 3(b) (black line). The temporal phase is also depicted in Figure 3(b) (red line). This generates a pulse compression factor of 3.86. The limited pulse compression ratio is primarily due to the low transmission of the FS plates. We attempted to set the MPC to 51 passes, which only slightly broadens the spectrum compared to 41 passes, but reduces the efficiency to approximately 74%. By integration, we estimate that about 81.4% of the pulse energy is concentrated in the main peak. This value is clearly lower than the FTL pulse, which we attribute to the uncompensated high-order dispersion, which arises from the grating compressor of the driving laser. Also, chirped pulses experiencing SPM broadening may accumulate unwanted high-order dispersion[24]. Thus, commercially available standard chirped mirrors have difficulty in compressing pulses to the FTL[27].

To compare the results of spectral broadening and pulse compression after introducing positive or negative dispersion, the pulse duration of the driving laser is pre-chirped to 600 fs by introducing negative dispersion before injection into the MPC unit. Under these conditions, pulse propagation in the MPC initially experiences spectral compression and then subsequent spectral broadening[28]. The evolution of the spectra as the pulse propagates in the MPC is illustrated in Figure 4. As the laser pulse passes the FS plates once, the spectral bandwidth quickly narrows to 7.5 nm, as shown in Figure 4(b). After propagating six times in the MPC unit, the spectral bandwidth narrows to a minimum of 3.8 nm, as shown in Figure 4(g). The spectral broadening occurs from the seventh pass, as shown in Figure 4(h), with an increase in intensity of the newly generated side lobes, marked with a red circle.

After 41 passes, dramatic spectral broadening is realized, as shown in Figure 5(a) (red line). It has a spectral bandwidth of 49.6 nm (taken from half the intensity of the outer spectral maximum), which is narrower than the broadened spectrum (63.1 nm) when the pulse is positively pre-chirped, as mentioned previously. In addition, the shape of the broadened spectrum after the pulse is positively and negatively pre-chirped is clearly different. The spectral intensity of the blue side is apparently lower than that of the red side, which suggests the spectral broadening at the negatively pre-chirped condition mainly arises from SPM and self-steeping[29]. The FTL of the broadened spectrum (negatively pre-chirped) is calculated to be 46.7 fs, as shown in the inset of Figure 5(b) (blue line). It is estimated that 91% pulse energy is concentrated in the main pulse. This value is slightly higher than the FTL pulse when the driving laser is positively pre-chirped. When the compensated GDD reaches –7600 fs^2, the temporal width of the pulse is compressed to 51 fs, as shown in Figure 5(b) (black line). The temporal

https://doi.org/10.1017/hpl.2024.67 Published online by Cambridge University Press

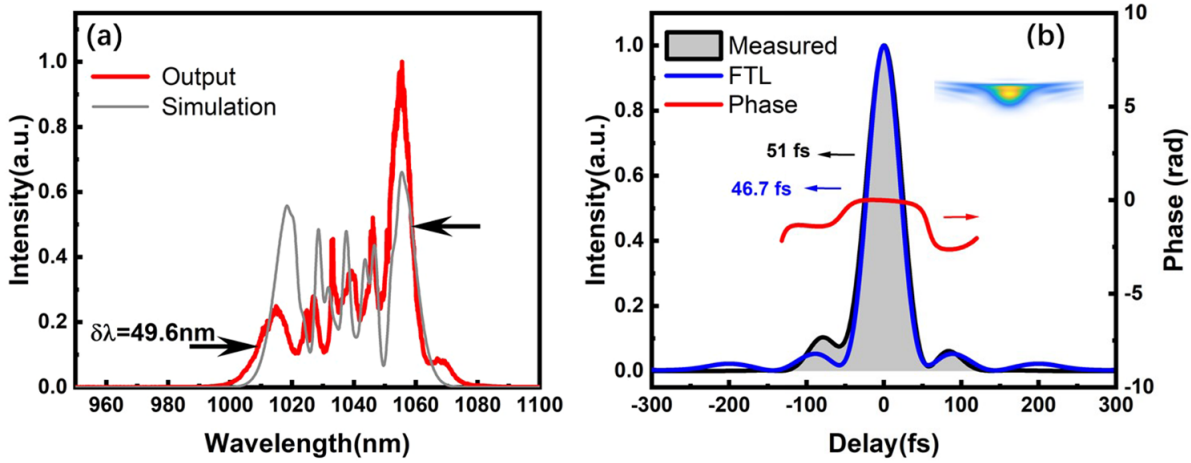

Figure 5. (a) Spectrum after negatively pre-chirped MPC and of simulated broadened spectrum. (b) Black line, retrieved temporal intensity; red line, retrieved phase; blue line, FTL; inset, measured FROG trace.

Table 1. Properties of the pre-chirp managed MPC at different chirp signs.

Chirp sign	Spectral bandwidth (nm)	FTL (fs)	Pulse duration (fs)	GDD (fs^2)	Fraction of energy in the main peak (%)
Positive	63.1	43.3	44	–6200	81.4
Negative	49.6	46.7	51	–7600	89.0

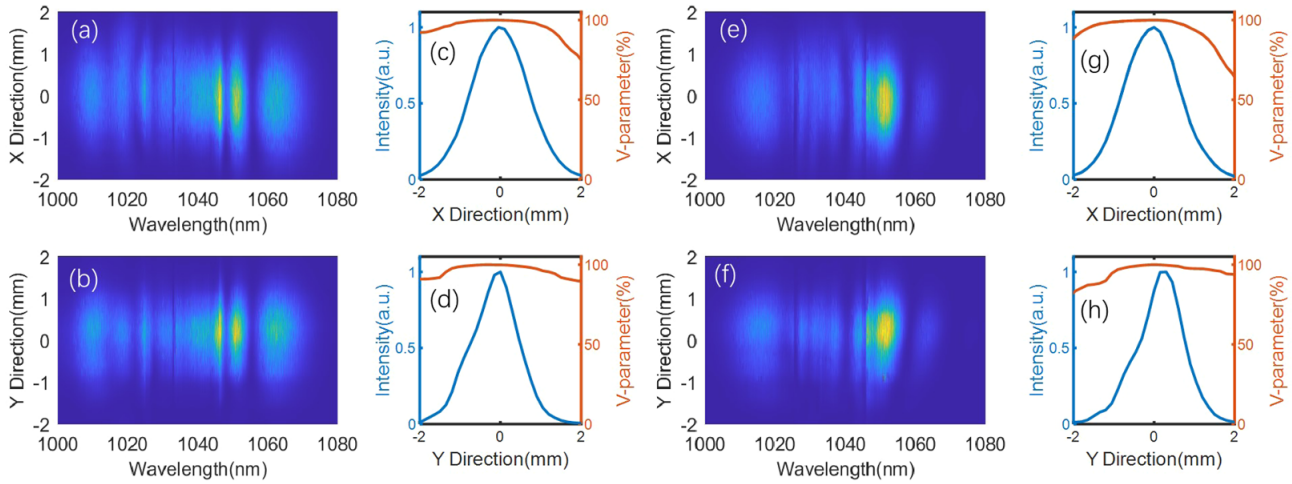

Figure 6. Spatio-spectral homogeneity characterization of the compressed pulse for positively (a), (b) and negatively (e), (f) pre-chirped conditions. (c), (d) and (g), (h) show the intensity distribution and corresponding V-parameter of both directions for two pre-chirped conditions. The blue curves show the normalized intensity of the spectral profile. The red curves show the spatial-spectral homogeneity values (V-parameter).

phase is also depicted in Figure 5(b) (red line). Hence, the available compressed pulse duration for the negatively pre-chirped condition is longer than that for the positively pre-chirped condition in our experiment. These experimental results are summarized in Table 1.

The spatio-spectral homogeneity of the laser beam is characterized by measuring the spectra every 200 μm across the transverse profile of the compressed beam for both positively pre-chirped and negatively pre-chirped conditions, as depicted in Figure 6. In the positively pre-chirped condition shown in Figures 6(c) and 6(d), the V-parameter (defined by Weitenberg *et al.*[30]) conditions are over 89% (X direction) and 95% (Y direction) within a beam diameter ($1/e^2$). By weighting the overlap with the intensity, effective overlaps of $V_X = 98.2\%$ and $V_Y = 99.5\%$ are calculated. In the negatively pre-chirped condition shown in Figures 6(g) and 6(h), the V-parameter exceeds 88% (X direction) and 95% (Y direction) within a beam diameter ($1/e^2$). As a result, $V_X = 97.9\%$ and $V_Y = 98.5\%$ are calculated. Therefore, we conclude that the spatial chirp resulting from the pre-chirped MPC unit is relatively weak.

The power stabilities before and after the positively pre-chirped managed MPC device are characterized. Power measurements were taken at a frequency of 10 points per second

https://doi.org/10.1017/hpl.2024.67 Published online by Cambridge University Press

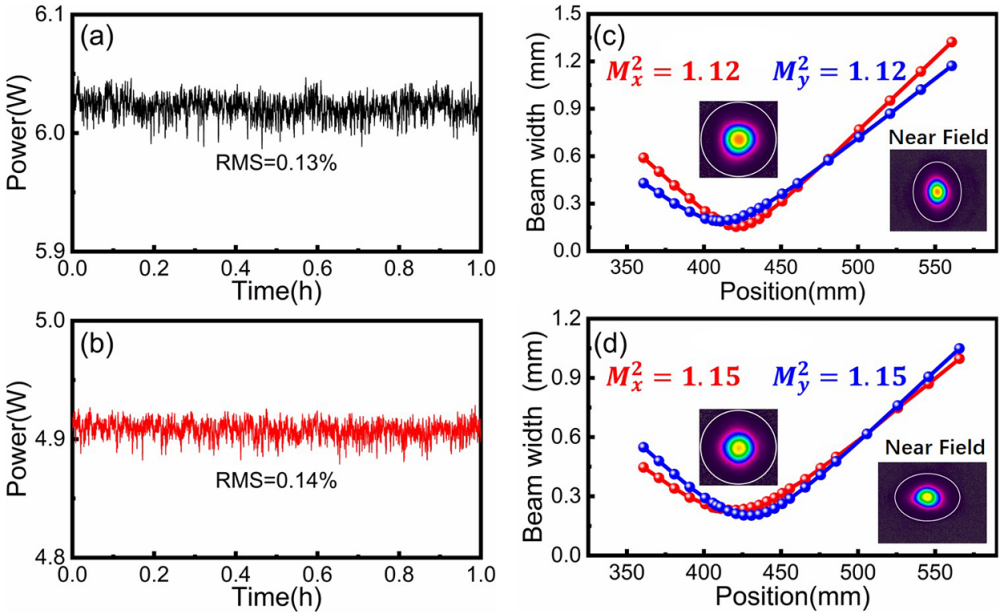

Figure 7. Power stability before (a) and after (b) the positively pre-chirped MPC unit. (c) Beam quality of the driving laser. (d) Beam quality after the positively pre-chirped MPC unit.

and are shown in Figures 7(a) and 7(b). The root mean square (RMS) stabilities of the laser power before and after the MPC unit are 0.13% and 0.14%, respectively. The beam quality factors before and after the MPC are measured to be $M^2 = 1.12 \times 1.12$ and $M^2 = 1.15 \times 1.15$, respectively, as shown in Figures 7(c) and 7(d). It is clear that the pre-chirp managed solid-state MPC device can address GW-level laser pulses while preserving the power stability and beam quality.

In summary, post-compression of the GW-level laser pulse in a solid-state MPC using the pre-chirp managed approach is demonstrated. When the pulse is positively pre-chirped, the spectrum broadens to 63.1 nm and the pulse compresses to 44 fs. Spectral compression and subsequent spectral broadening are observed as the negatively pre-chirped pulse propagates through the MPC. The resulting broadened spectral bandwidth is 49.6 nm and the compressed pulse duration is 51 fs. The power stability and beam quality after the MPC unit are almost preserved. The transmission efficiency of our MPC device is 81%. This efficiency is slightly lower for a single-stage solid-state MPC device, mainly due to the low transmittance of the FS plates. Assuming the reflectivity/transmission of the MPC mirrors and FS plates reaches 99.99%, the FTL pulse duration supported by the broadened spectrum is about 26 fs, achieving an efficiency greater than 94% using a scheme similar to the one described by Song *et al.*[31]. In addition to the pre-chirp management method, divided-pulse nonlinear compression can also enhance the handling capability of post-compression devices[23]. By incorporating these techniques into a solid-state MPC, it is possible to post-compress multi-GW laser pulses.

Acknowledgements

This work was supported by the National Natural Science Foundation of China (Nos. 12388102, 62205351, 61925507, 62075227 and 22227901), the Youth Innovation Promotion Association CAS (No. 2020248), the Shanghai Sailing Program (No. 20YF1455000) and the Shanghai Rising-Star Program (No. 21QA1410200).

References

1. E. Lorek, E. W. Larsen, C. M. Heyl, S. Carlstrom, D. Palecek, D. Zigmantas, and J. Mauritsson, Rev. Sci. Instrum. **85**, 123106 (2014).
2. A.-L. Viotti, C. Li, G. Arisholm, L. Winkelmann, I. Hartl, C. M. Heyl, and M. Seidel, Opt. Lett. **48**, 984 (2023).
3. M. A. van Dijk, M. Lippitz, D. Stolwijk, and M. Orrit, Opt. Express **15**, 2273 (2007).
4. P. A. Mante, S. Lehmann, D. F. Shapiro, K. Lee, J. Wallentin, M. T. Borgstrom, and A. Yartsev, ACS Photonics **7**, 1923 (2020).
5. G. D. Zhang and G. H. Cheng, Appl. Opt. **54**, 8957 (2015).
6. X. W. Cao, Q. D. Chen, H. Fan, L. Zhang, S. Juodkazis, and H. B. Sun, Nanomaterials **8**, 287 (2018).
7. S. Bohman, A. Suda, T. Kanai, S. Yamaguchi, and K. Midorikawa, Opt. Lett. **35**, 1887 (2010).
8. C. H. Lu, Y. J. Tsou, H. Y. Chen, B. H. Chen, Y. C. Cheng, S. D. Yang, M. C. Chen, C. C. Hsu, and A. H. Kung, Optica **1**, 400 (2014).
9. P. He, Y. Y. Liu, K. Zhao, H. Teng, X. K. He, P. Huang, H. D. Huang, S. Y. Zhong, Y. J. Jiang, S. B. Fang, X. Hou, and Z. Y. Wei, Opt. Lett. **42**, 474 (2017).
10. M. Seo, K. Tsendsuren, S. Mitra, M. Kling, and D. Kim, Opt. Lett. **45**, 367 (2020).
11. J. Schulte, T. Sartorius, J. Weitenberg, A. Vernaleken, and P. Russbueldt, Opt. Lett. **41**, 4511 (2016).

https://doi.org/10.1017/hpl.2024.67 Published online by Cambridge University Press

12. J. Weitenberg, A. Vernaleken, J. Schulte, A. Ozawa, T. Sartorius, V. Pervak, H. D. Hoffmann, T. Udem, P. Russbuldt, and T. W. Hansch, Opt. Express **25**, 20502 (2017).
13. M. Kaumanns, V. Pervak, D. Kormin, V. Leshchenko, A. Kessel, M. Ueffing, Y. Chen, and T. Nubbemeyer, Opt. Lett. **43**, 5877 (2018).
14. C. Grebing, M. Muller, J. Buldt, H. Stark, and J. Limpert, Opt Lett **45**, 6250 (2020).
15. M. Kaumanns, D. Kormin, T. Nubbemeyer, V. Pervak, and S. Karsch, Opt. Lett. **46**, 929 (2021).
16. W. Liu, C. Li, Z. G. Zhang, F. X. Kartner, and G. Q. Chang, Opt. Express **24**, 15328 (2016).
17. W. Liu, S. H. Chia, H. Y. Chung, R. Greinert, F. X. Kartner, and G. Q. Chang, Opt. Express **25**, 6822 (2017).
18. F. Emaury, C. J. Saraceno, B. Debord, D. Ghosh, A. Diebold, F. Gerome, T. Sudmeyer, F. Benabid, and U. Keller, Opt. Lett. **39**, 6843 (2014).
19. F. Guichard, A. Giree, Y. Zaouter, M. Hanna, G. Machinet, B. Debord, F. Gerome, P. Dupriez, F. Druon, C. Honninger, E. Mottay, F. Benabid, and P. Georges, Opt. Express **23**, 7416 (2015).
20. M. Hanna, F. Guichard, N. Daher, Q. Bournet, X. Délen, and P. Georges, Laser Photonics Rev. **15**, 2100220 (2021).
21. A.-L. Viotti, M. Seidel, E. Escoto, S. Rajhans, W. P. Leemans, I. Hartl, and C. M. Heyl, Optica **9**, 197 (2022).
22. L. Lavenu, M. Natile, F. Guichard, Y. Zaouter, X. Delen, M. Hanna, E. Mottay, and P. Georges, Opt. Lett. **43**, 2252 (2018).
23. H. Stark, C. Grebing, J. Buldt, A. Klenke, and J. Limpert, J. Phys. Photonics **4**, 035001 (2022).
24. R. Z. Chen and G. Q. Chang, J. Opt. Soc. Am. B **37**, 2388 (2020).
25. A. K. Raab, M. Seidel, C. Guo, I. Sytcevich, G. Arisholm, A. L'Huillier, C. L. Arnold, and A. L. Viotti, Opt. Lett. **47**, 5084 (2022).
26. J. M. Dudley, G. Genty, and S. Coen, Rev. Mod. Phys. **78**, 1135 (2006).
27. E. Escoto, A.-L. Viotti, S. Alisauskas, H. Tünnermann, I. Hartl, and C. M. Heyl, J. Opt. Soc. Am. B **39**, 1694 (2022).
28. M. Oberthaler and R. A. Hopfel, Appl. Phys. Lett. **63**, 1017 (1993).
29. T. Nagy, P. Simon, and L. Veisz, Adv. Phys. X **6**, 1845795 (2021).
30. J. Weitenberg, A. Vernaleken, J. Schulte, A. Ozawa, T. Sartorius, V. Pervak, H. D. Hoffmann, T. Udem, P. Russbüldt, and T. W. Hänsch, Opt. Express **25**, 20502 (2017).
31. J. Song, L. Shen, J. Sun, Z. Wang, Z. Wei, Y. Peng, and Y. Leng, Opt. Express **30**, 24276 (2022).

https://doi.org/10.1017/hpl.2024.67 Published online by Cambridge University Press